Mohammed Yassine Dennai*[1], Hamza Tedjini[1], Abdelfatah Nasri[1], Djamel Taibi[2]

Smart Grids & Renewable Energies Laboratory (SRGE), Faculty of Technology, University of Tahri Mohammed Bechar, Algeria (1)
University of Kasdi Merbah Ouargla, Route de Ghardaia, BP.511, 30 000, Algeria (2)

doi:10.15199/48.2021.03.25

MPC controller of PV system based Three-Level NPC Inverter under different climatic conditions connected to the grid

***Abstract**. In this paper, PV arrays are connected to the grid through a three-Level NPC Inverter. Both the current control and voltage balancing performance of the inverter are ensured via model predictive control (MPC) technique. This paper is comparing and presenting operational performance analysis of grid-connected three-Level NPC Inverter results using three techniques controllers namely: Self-tuning Fuzzy Logic PI controller (FLC), Neural Network controller (ANN), and PI classical controller, under different environmental conditions to optimally tune the reference current of the controller and following the maximum power point.*

***Streszczenie.** Opisano system ze źródłem fotowoltaicznym gdzie stosuje się zarówno bieżące operacje kontroli, jak i równoważenie napięcia NPC z porównaniem trzech różnych strategii kontrolera. Skuteczność porównuje się między trzema strategiami kontrolnymi przy różnym natężeniu promieniowania i różnej temperaturze. (**Analiza wydajności trójpoziomowego falownika NPC podłączonego do sieci przy użyciu sterownika MPC w różnych warunkach klimatycznych**).*

Keywords: NPC inverter, Model predictive control (MPC), ANN, P&O algorithm.
Słowa kluczowe: Falownik NPC, sterowanie predykcyjne , ANN, algorytm P&O.

Introduction

Among the different solar technologies available, photovoltaic PV systems are seen as promising. This photovoltaic system can be handled either by the storage system or in grid-tied mode [6, 22]. To increase the DC voltage, Grid-connected systems should be installed with series-connected PV modules. The common energy of the photovoltaic systems can be transferred to the grid using multi-level DC / AC inverters without needing to the transformer. These multilevel inverters received great significant attention due to its broad range of applications in industry as a neutral point clamped converter (NPC), flying condenser converter (FCC), and cascaded H-bridge (CHB) converter [4, 5].

In high power applications and transformerless power conversion systems, multi-level NPC inverters are preferred because the installation costs are reduced, have small filters, have low harmonic effects, and can be used at high voltage. Nowadays, there are many different control techniques that have been proposed as sliding mode control, decoupling control [11, 12], hysteresis control, and MPC [13, 14]. Model predictive control has many advantages that are proper for the control of power converters, direct generation of PWM signals, the controller resulting is simple to implement, and there is no need for a modulator. In addition, the voltage balance control among the input capacitors is given from the MPC simply without needing additional circuits [20].

In this paper, produced power has been transferred to the grid using the NPC inverter, which is controlled using the MPC algorithm with the overcome the problem of voltage balancing. Perturb & Observe (P&O) is the proposed MPPT controller which defines the reference voltage (Vdc_ref) value of the inverter and the control strategies shape the inverter reference current (Idc_ref). Moreover, three techniques strategies to control the PV system are applied, the first using a PI controller, the second using a Self-tuning fuzzy logic controller, and the third with an ANN controller. In this work, The ANN generates a reference current in different weather parameters G and T. The ANN controller is developed in two modes: offline mode, which is required to test different sets of neural network parameters to find the optimal neural network controller (structure, trigger function, and learning algorithm), and online mode is the optimal ANN controller used in this system. The proposed neural network controller is tested and validated for various conditions using MATLAB/Simulink model. So, the proposed ANN controller has a good performance response process. The comparative study shows that the performance with the fuzzy logic controller is slightly better than that with a simple PI controller.

System description

The proposed system model of a three-phase grid-tied inverter is shown in Fig. 1. As can be seen in this figure, the proposed system comprises of PV panel group, the three-level NPC inverter, the phase locked loop (PLL) circuit, the LC filter, the P&O based MPP technique and the block strategy controller. PV panel group is directly connected to grid through a three-phase inverter. The PLL is utilized to provide the synchronization of the output current of NPC inverter with the grid voltage. The output of the P&O MPPT technique sets the reference voltage (Vdc_ref), this reference voltage is compared with the measured value of the input voltage of NPC (Vdc_in), and the error is processed by one of proposed control strategies to generate required reference current (Idc_ref). This reference current is transformed into (abc) coordinates via the inverse Park transformation and PLL to obtain the three-phase current reference (Idc_ref), (Ia^*, Ib^*, Ic^*) of the MPC. Then the MPC is used to generate the required pulses to control the NPC inverter and ensure the balance of input voltage.

Three Level NPC Inverter and Model Predictive Control

The neutral point clamped converters are commonly used for medium voltage power applications [12]. The configuration of three phase NPC converter is shown in Fig. 1. Each phase of inverter is included of 4 switching devices series connected controlled semiconductor power switches with antiparallel diodes and two clamping diodes [1]. The load parameters are composed of inductance L, resistance R and electromotive force of the load (EMF) e with e_a, e_b and e_c of three-phase load. The leg voltages generated by inverter can be defined:

$$V_{xo} = S_x \frac{V_{dc}}{2} \quad \text{where: } x = \{a, b, c\} \tag{1}$$

where V_{dc} is the DC link input voltage and the switching function represented the states of each leg, which specified according to the switching signals of each leg, as cleared in (2):

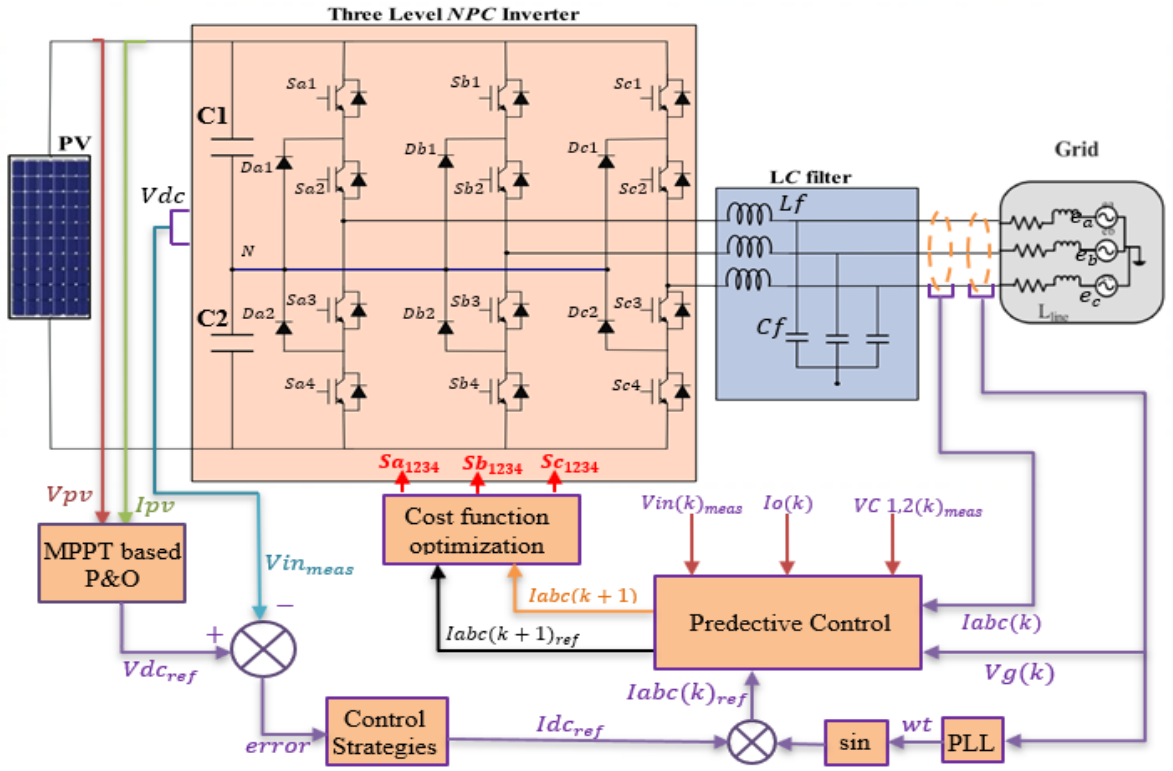

Fig.1. The general model of the proposed system

(2) $$S_x \begin{cases} 1 & if \;\; S_{x1}=on \;\; ,S_{x2}=on \;\; ,S_{x3}=off \;\; ,S_{x4}=off \\ 0 & if \;\; S_{x1}=off \;\; ,S_{x2}=on \;\; ,S_{x3}=on \;\; ,S_{x4}=off \\ -1 & if \;\; S_{x1}=off \;\; ,S_{x2}=off \;\; ,S_{x3}=on \;\; ,S_{x4}=on \end{cases}$$

The combination of three states 1, 0, and -1 produces 27 switching states including 19 space voltage vectors for the three-phase three-level inverter, as shown in Fig. 2. The output load current prediction for the system in Fig. 1 is obtained as [10, 24, 25]:

(3) $$L\frac{di}{dt} = v - Ri - e$$

where R and L are the load resistance and inductance respectively, v is the voltage vector generated by the inverter, e is the electromotive force of the load and i is the load current vector. The current and voltage vectors are defined by:

(4) $$v = \frac{2}{3}\left(V_{ao} + aV_{bo} + a^2V_{co}\right)$$

(5) $$i = \frac{2}{3}\left(i_a + ai_b + a^2i_c\right)$$

(6) $$e = \frac{2}{3}\left(e_a + ae_b + a^2e_c\right)$$

where: $a = e^{j\frac{2\pi}{3}}$

The discrete time model of the system is used to predict the future values of the controlled variable using the measured system parameters at the sampling instant [2]. A forward Euler method (7) can be used to determine the future line-current prediction of the NPC inverter considering all possible voltage vectors with the sampling period T_S:

(7) $$\frac{di(t)}{dt} \approx \frac{i(k+1)-i(k)}{T_S}$$

Replacing (7) in (3) to get predictions for the future value of the line current vector $i(k+1)$:

(8) $$i(k+1) = \left(1 - \frac{RT_S}{L}\right)i(k) + \frac{TS}{L}\left(v(k) - e(k)\right)$$

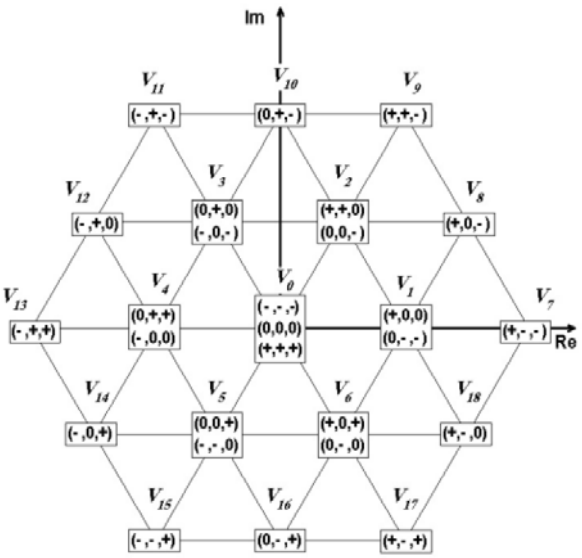

Fig.2. Voltage vectors for a three-level NPC inverter with the possible switching states

Applying similar method and assumptions for the estimation of the load back-emf from (8) resulting in the following expression:

(9) $$e(k-1) = v(k-1) - \frac{L}{T_S}i(k) - \left(R - \frac{L}{T_S}\right)i(k-1)$$

For a sufficiently small sampling time, it is possible to consider $e(k-1) \approx e(k)$, so no extrapolation is needed.

Since switching states with the same voltage vector will produce a different effect on the charge or discharge of the DC link capacitors, this prblem causes The of DC-link capacitors unbalance voltage [1]. As can be seen in Fig. 1, The dynamics of the DC-link capacitor voltages are described by the capacitor differential equations:

(10) $$\frac{dv_{c1}}{dt}=\frac{1}{C_1}i_{c1}$$

(11) $$\frac{dv_{c2}}{dt}=\frac{1}{C_2}i_{c2}$$

where C_1 and C_2 are the capacitor values. Using the same previous steps as the discrete-time equation for the current can be described the prediction of capacitor voltage values at the sampling $k+1$ as:

(12) $$Vc_1(k+1)=Vc_1(k)+\frac{Ts}{C_1}ic_1(k)=Vc_1(k)+\frac{T_S}{2.C_1}i_o(k)$$

(13) $$Vc_2(k+1)=Vc_2(k)+\frac{Ts}{C_2}ic_2(k)=Vc_2(k)-\frac{T_S}{2.C_2}i_o(k)$$

where: VC_1 and VC_2 dc-link capacitor voltages, i_{C1} and i_{C2} currents through each dc-link capacitor and i_o current via the dc-link midpoint.

The current through the dc-link midpoint i_o can be determined using (14), which depend on the inverter's switching states from (2) and the present current values of three phase i_a, i_b and i_c [3, 21].

(14) $$i_o(k)=S_{ao}(k).i_a(k)+S_{bo}(k).i_b(k)+S_{co}(k).i_c(k)$$

where: $S_{xo}=\begin{cases}1 & if\ \ S_x=0\\ 0 & Otherwise\end{cases}\ ;\ x=\{a,b,c\}$

Cost Function Optimization

For Choosing the cost function is a key part of the MPC technique. The proposed MPC scheme consist of two cost functions that are used to minimize output current and capacitor voltage errors in the next sampling time.

The cost functions of the output currents and capacitor voltage are:

(15) $$\begin{aligned}g_i &=\| i_j^*(k+1)-i_j(k+1)\|^2\\ &=[i_b^*(k+1)-i_b(k+1)]^2+\\ &\quad [i_b^*(k+1)-i_b(k+1)]^2+\\ &\quad [i_c^*(k+1)-i_c(k+1)]^2.\end{aligned}$$

(16) $$g_v=\lambda\,|\,v_{C1}(k+1)-v_{C2}(k+1)\,|^2$$

Where $i_j^*(k+1)$ and $i_j(k+1)$ are the reference and predictive output current vector respectively in the next step ($j=a,b,c$). $v_{C1}(k+1)$ and $v_{C2}(k+1)$ are the predective DC link capacitor voltages respectively and λ is the weighting factor. The full cost function is:

(17) $$g(k+1)=g_i(k+1)+g_v(k+1)$$

MPPT P&O Technique

For its simplicity and ease of implementation, the P&O algorithm is one of the most commonly used algorithms for PV systems (MPPT methods). [2, 7-9]. Where, it consists in disturbing the voltage V_{PV} of a small amplitude around its initial value and analysed the change in power P_{PV} which results from it as well to determine the change direction. Fig. 3 shows the flow chart of the classic algorithm. In this method, the voltage of the solar panel is slightly disturbed (increase or decrease) then the PV output power $P(k)$ is compared with the previous power disturbance $P(k-1)$. If the output power is increased, the following disturbance will be made in the same direction. If the output power is decreased, a novel disturbance is generated in the opposite direction.

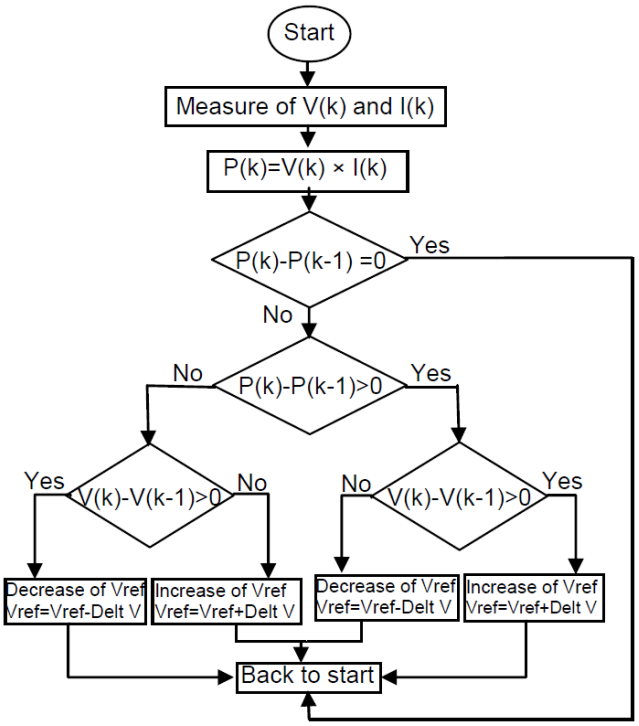

Fig.3. Flowchart diagram of the classical P&O algorithm

Control Strategies of the System

Self-tuning Fuzzy PI controller

Fuzzy logic controller is a Mamdani type [19]. In the Fig. 4, the error ε between Vdc_ref and Vdc_meas is the input of a Fuzzy PI controller which output is the estimated reference current (Idc_ref). This estimated reference current is used in the predictive current control (MPC) algorithm.

As showing in Fig. 4, The fuzzy inference system has two inputs and two outputs. The input variables are the error e and the rate of change of the error e_c, and the output variables are ΔK_p and ΔK_i. Their values are corrected according on a set of rules. The following formula can be used to obtain the proportional coefficient K_p and the integral coefficient K_i:

(18) $$k_p=k_{p0}+\Delta k_p$$

(19) $$k_i=k_{i0}+\Delta k_i$$

where K_{p0} and K_{i0} are the reference values obtained through experiments such as: $k_{p0}=0.6258$, $k_{i0}=0.00744$.

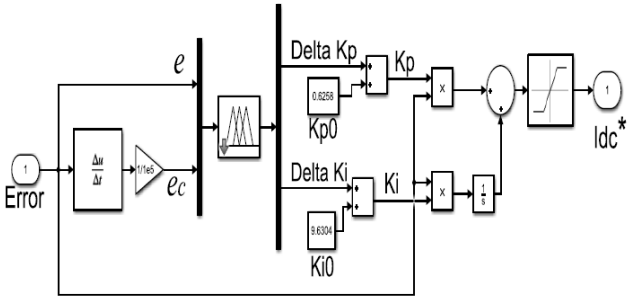

Fig.4. Self-tuning Fuzzy Logic PI controller

In Fig. 5 there are seven different membership functions are used for the input and output variables: NB, NM, NS, ZE, PS, PM, PB mean successively large negative, medium negative, small negative, zero, small positive, medium positive, and large positive.

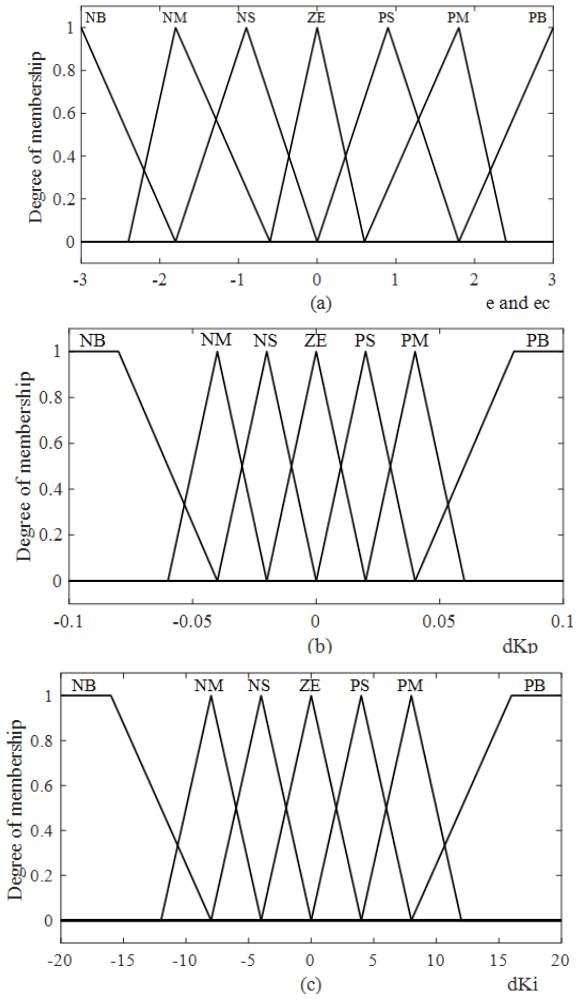

Fig.5. Membership functions of the input and output variables: (a) Membership function of the inputs variables e and e_c, (b) Membership function of output variable ΔK_p and (c) Membership function of output variable ΔK_i

Rules of The Fuzzy Logic Controller

Table 1. Fuzzy rules table of ΔK_p

e_c	e						
	NB	NM	NS	ZE	PS	PM	PB
NB	NB	NB	NB	NB	NM	NS	ZE
NM	NB	NB	NB	NM	NS	ZE	PS
NS	NB	NB	NM	NS	ZE	PS	PM
ZE	NB	NM	NS	ZE	PS	PM	PM
PS	NM	NS	ZE	PS	PM	PB	PB
PM	NS	ZE	PS	PM	PB	PB	PB
PB	ZE	PS	PM	PB	PB	PB	PB

Table 2. Fuzzy rules table of ΔK_i

e_c	e						
	NB	NM	NS	ZE	PS	PM	PB
NB	NB	ZE	ZE	PM	ZE	ZE	NS
NM	NM	NS	ZE	PS	ZE	NS	NM
NS	NB	NM	ZE	PS	ZE	NM	NB
ZE	NB	NB	NS	ZE	NS	NB	NB
PS	NB	NM	ZE	PS	ZE	NM	NB
PM	NM	NS	ZE	PS	ZE	NS	NM
PB	NS	ZE	ZE	PM	ZE	ZE	NS

The proposed ANN controller

The neural network is used for optimum values and then the optimum values are used for the training network. ANN is trained periodically, wherefore, each PV system should be achieved the desired data for the training process [15-18]. In this work, the neural network controller is used to estimate the optimum reference current (*Idc_ref*), which corresponds to the maximum power at any given irradiation levels and temperature. The input variables are temperature T, solar radiation G, V_{mpp} corresponding to MPP, V_{in} corresponding to the input voltage of NPC and the previous reference current *Idc_ref(k-1)*. And the reference current (*Idc_ref*) is the output variable of ANN as shown in Fig. 6. Four layers can be considered for the proposed ANN controller, which has three layers, first, second and third layers have 9, 3, and 7 neurons, respectively and the fourth layer has 1 neuron. The first and second layers of the transfer functions are logsig, the third and fourth layers are choosing randomly. Training ANN is carried out in 300 iterations that it will converge to a required target. The characteristic proposed ANN controller is displayed in Fig. 7. In order to train the neural network, 200 data are used (irradiance between 0.1 to 1 kilowatt per square meter (KW/m^2), temperatures between 10° C to 55° C, a set of 200 for each of V_{mpp} corresponding to MPP, V_{in} corresponding to the input voltage of NPC and the previous reference current *Idc_ref(k-1)*) and also, a set of 200 the reference current (*Idc_ref*) is obtained by PI Fuzzy logic controller.

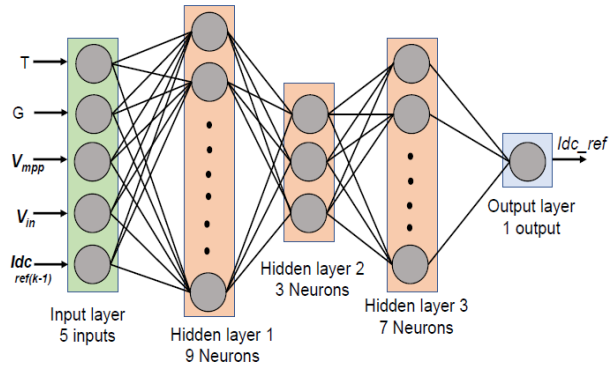

Fig.6. The proposed artificial neural network controller

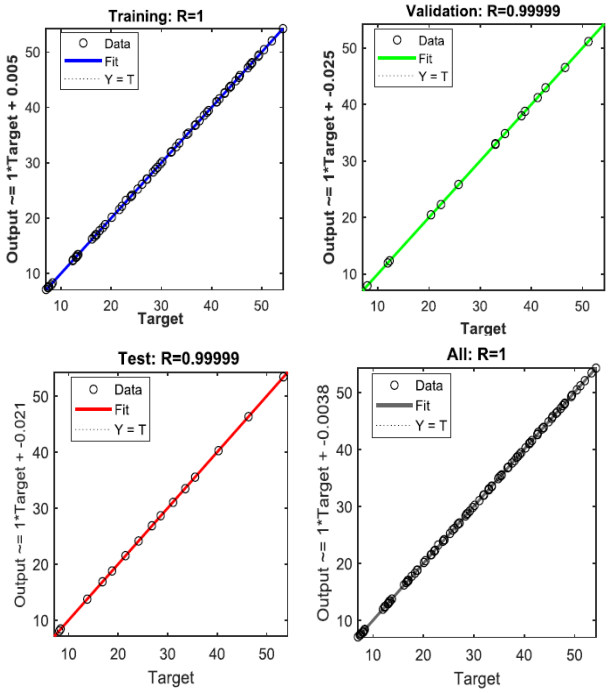

Fig.7. Characteristics proposed ANN control

LC Filter Design

The LC filter is used as the interface among the inverter and the power grid. By perfectly designed, a high-quality grid current is achieved [26]. Therefore, the design requires the following parameters:

$$C_f = \frac{0.05 \times P_n}{2 \times \pi \times f_g \times V_g} \tag{20}$$

$$L_f = \frac{0.1 \times V_g^2}{2 \times \pi \times f_g \times P_n} \tag{21}$$

Where, P_n : nominal output power, V_g : Inverter phase to phase RMS voltage, f_g : grid frequency and f_S : switching frequency. These values are given in Table 3.

Results and Discussions

The proposed system scheme is simulated in MATLAB/Simulink to validate the efficacy of the system. The parameters used in the simulation are shown in Table 3 and the proposed system has been tested under the three different controllers (Self tuned Fuzzy PI, Neural network controller, and PI controller), into account the insolation and temperature variations. The classical P&O algorithm has been used with each of the three previous controllers.

Table 3. The parameters of the sensor

Variables and Parameters	Values	Units
Three-phase Grid Voltage	380 (rms)	V
Number of panels (in parallel)	4	
Number of panels (in series)	27	
Total PV output power (P)	23	kW
Grid Frequency	50	Hz
Vdc nominal	783	V
C1 and C2 capacitors	1500	µF
Filter Inductance	9.2	mH
Filter resistance	0.91	Ω
capacitor Filter	5.5	µF
Sampling time	100	µs

Fig. 8 shows the simulation results under the assumption that the insolation is constant at 1000 W/m^2 and the temperature variation takes the curve shown in Fig. 8 (a). Fig. 8(b) shows that the power generated by the PV array system using the three controllers (FLC, ANN, and PI). The figure gives an indication that the three regulators make the power generated by the photovoltaic modules very close to the maximum power during the temperature fluctuation. With a slight preference for the ANN controller. Fig. 8(c) shows the inverter output power in which the efficiency of all methods is excellent (over 95%). Fig. 8(d) shows the output PV voltage. The self-tuned Fuzzy PI controller (FLC) has been reduced the voltage peak relatively compared to the one in PI classical controller, two voltage peaks are observed corresponding respectively to the FLC (900 V) and the PI (935 V). As we can see from the waveforms of each technical the proposed ANN controller has a fast-transient response compared with the other two methods. It can be seen that Vdc_meas tracks accurately the Vdc_ref with the three methods.

In order to simulate the varying irradiation condition, the irradiation level was decreased from 1000 W/m^2 to 500 W/m^2 and then increased to 700 W/m^2, as shown in Fig. 9(a). It can be seen in in Fig. 9(b) the effect of the irradiance g over the PV current. PV current is strongly affected when there is less solar irradiance reaching the surface of PV panels. Fig. 9(c) shows the output power from the solar panel system with the three controllers mentioned previously under the considering of constant and uniform Temperature (T= 25°C) and the variation in solar irradiance. They are collected in one figure to be a clear comparison between the three controllers. This figure illustrates that the three tested controllers try to keep the PV output power at or near its maximum value.

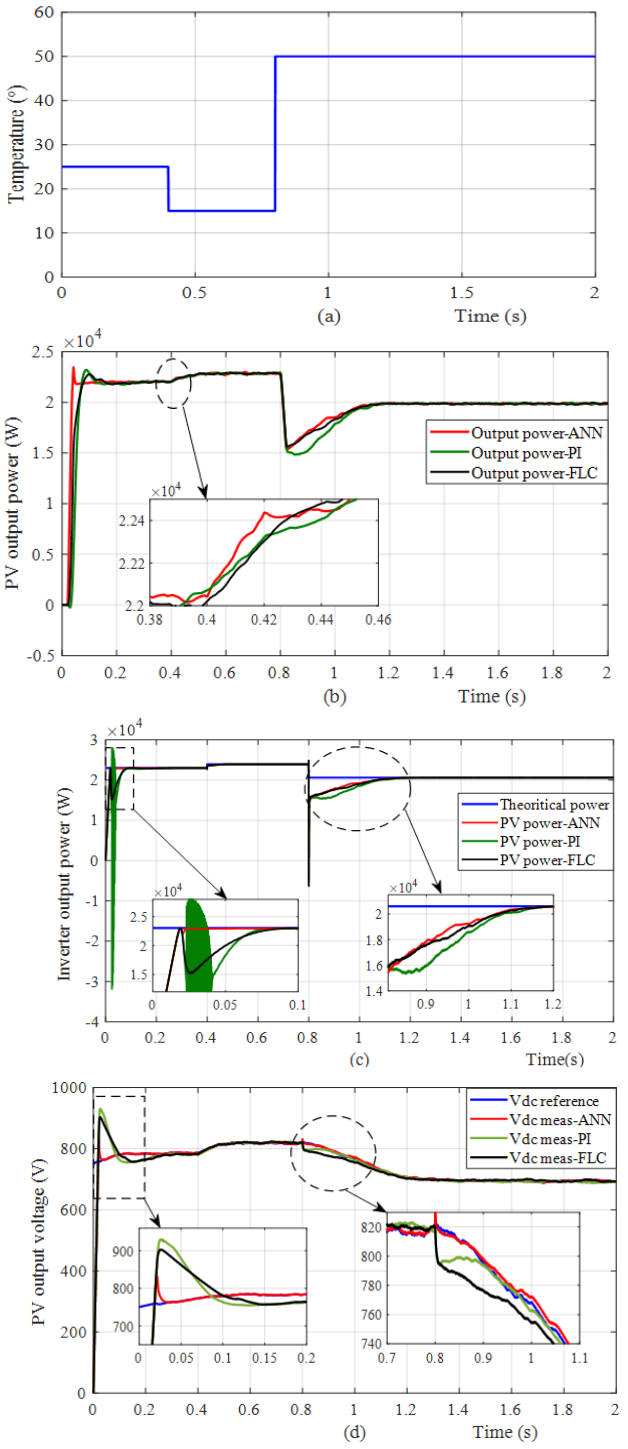

Fig.8. Simulation results under different temperature levels and constant insolation: (a) Temperature variation curve, (b) The panel output power, (c) The inverter output power and (d) The output PV voltage of each technical controller

When increasing or decreasing the irradiance level, the proposed ANN controller tracks the MPP quickly compared to FLC and PI and with slightly higher efficiency. Fig. 9(d) shows the inverter output power. In Fig. 9(e), it can be noticed that the three controllers are able to track the reference voltage Vdc_ref but the proposed ANN controller still has a fast response time even under nonuniform irradiance which is estimated at 15 ms, and less voltage peak than rest two controllers. The PV output voltage is not affected in the same amount compared to the PV output current.

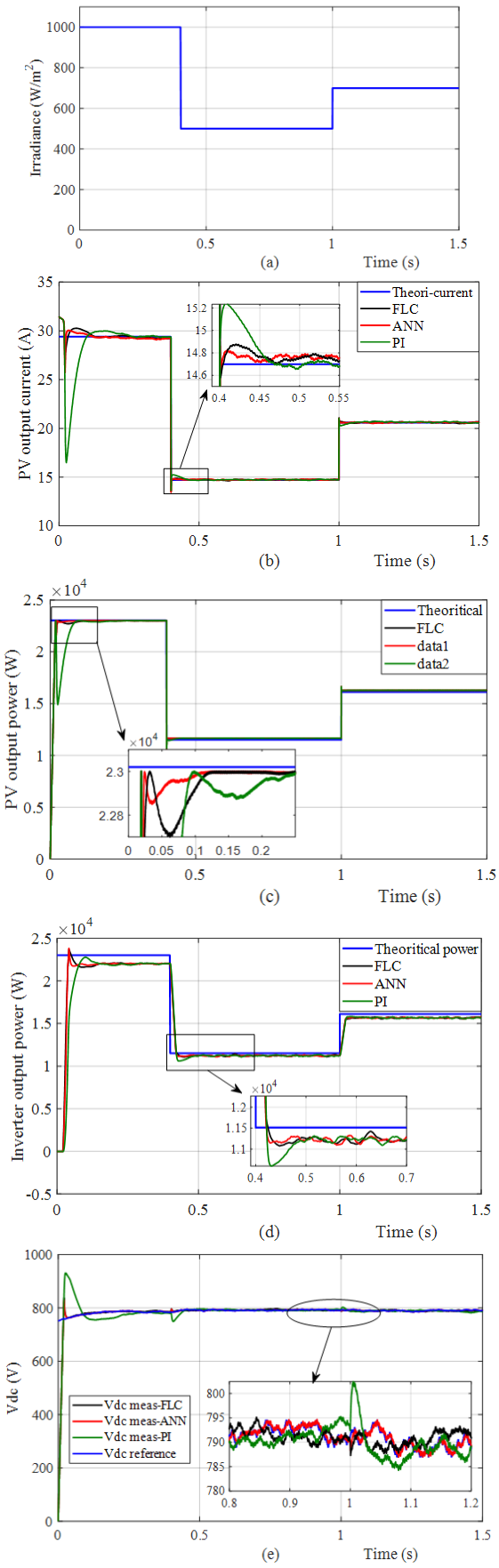

Fig.9. Simulation results under different irradiance levels and constant temperature.: (a) Solar insolation variation curve, (b) The panel output current, (c) The panel output power, (d) The inverter output power and (e) The output PV voltage of each technical controller

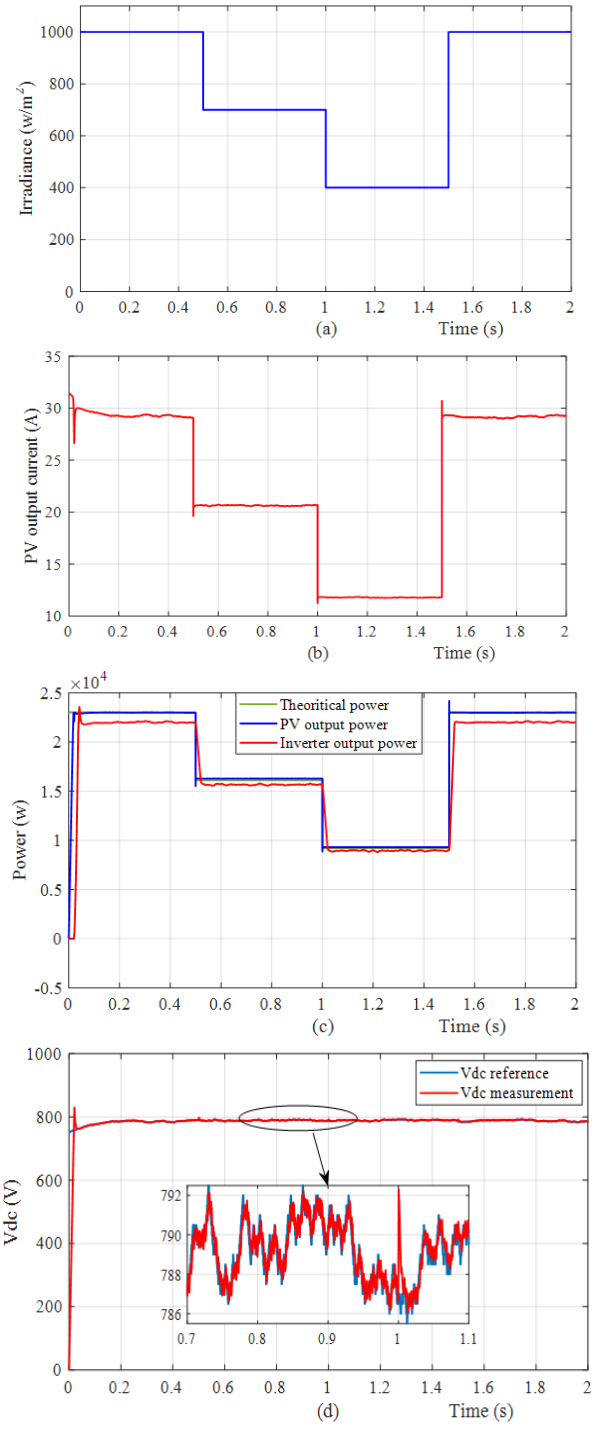

Fig.10. Simulation results by ANN controller: (a) Irradiance level, (b) Output power of: PV & Inverter, (c) PV output current, and (d) Output PV voltage *Vdc_mes* compared with reference voltage *Vdc_ref*

Additionally, a sudden change in the level of irradiance is used to test the performance of the proposed ANN controller. This irradiation profile will start at 1000 W/m^2, decreases at t=0.5 s to 700 W/m^2, which is down to 400 W/m^2 at t=1 s, and increases once more to 1000 W/m^2 at t=1.5 s. The temperature is considered constant at 25° C in whole this simulation process. Fig.10 shows, the solar irradiation level, the PV output power & Inverter output power, PV output current, and the PV output voltage compared with the reference voltage.

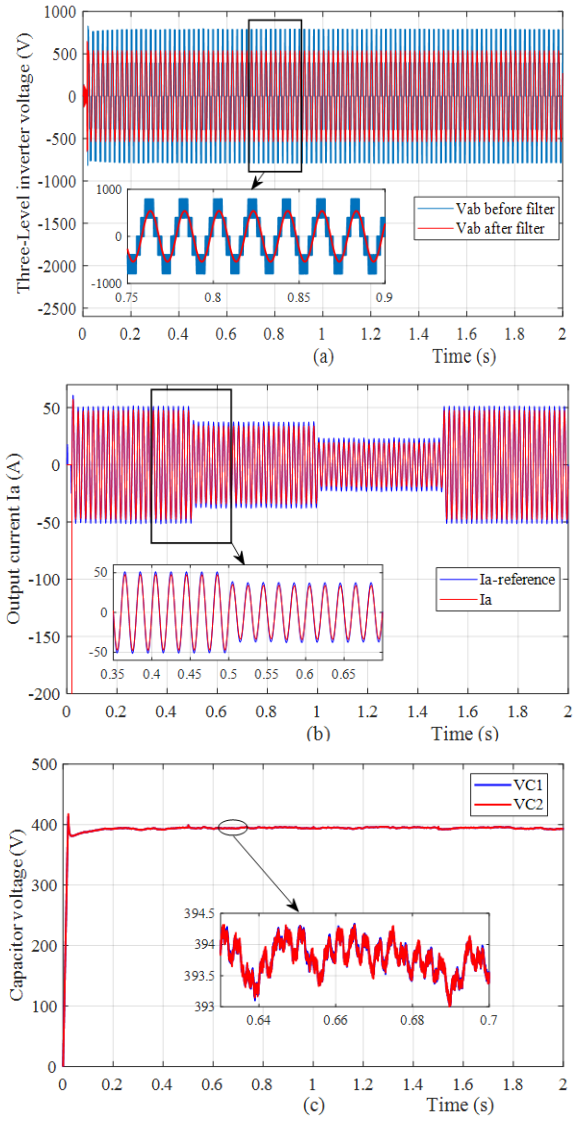

Fig.11. (a) Inverter output voltage before and after LC filter, (b) Current tracking with reference, and (c) Voltage balance across DC link voltage Vc1, Vc2 of the inverter

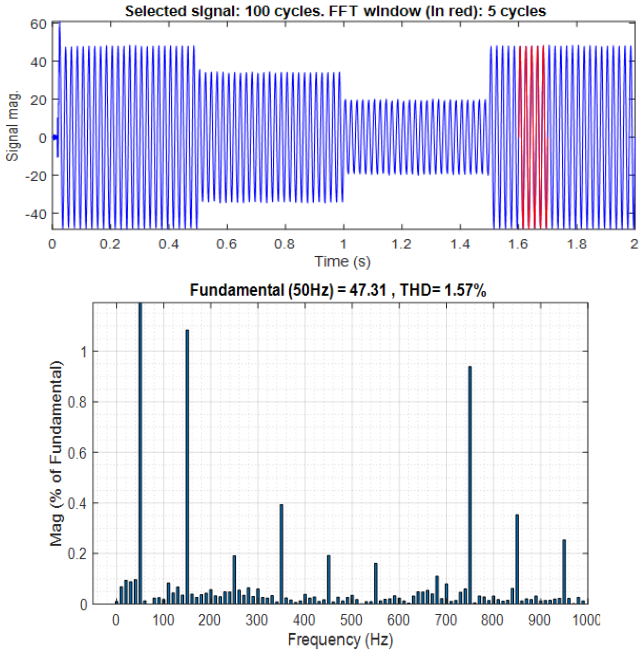

Fig.12. FFT analysis of the inverter output current

Fig. 11(a) illustrates the output line voltage of 3-level NPC inverter before and after LC filter. As we can see, the waveform is smoothed. Furthermore, the MPC algorithm effectively reduces the THD of the grid current by accurately tracking the sinusoidal reference current, which is presented in Fig. 11(b). Moreover, Fig. 11(c) confirms that the voltage balance between two dc-link capacitors voltage (VC1 and VC2) is accurately balanced by using the MPC algorithm. The value of the weighting factor is fixed at $\lambda = 0.001$.

Whereas, the FFT analysis of the output current of the inverter is shown in Fig. 12. The corresponding THD of this current is (1.57%) and it's within the acceptable range <5%.

Conclusion

This article contains a comparison between three different technical controls: Self tuned Fuzzy PI, Neural network controller, and conventional PI controller of multilevel PV system. The results show that all studied controllers are able to extract the maximum power from the solar system with different solar irradiation and temperatures from the photovoltaic cells.

All technical provide high efficiency under all examined conditions and showing ripples caused by oscillations around the MPP that reducing the value of the average output power (the efficiency depends on the level of the disturbance). The ANN controller extracts a higher average power under all conditions. Self-tuned Fuzzy PI and PI controller produce almost identical performance curves and similar performance.

Moreover, the control of power flow from the NPC inverter to the grid is assured by the developed MPC algorithm and with the LC filter. The reference current *Idc_ref* is set by the proposed MPPT (P&O), and one of three different controllers is used to extract the highest possible power from the PVs at all times. Additionally, the output current of the inverter has a nearly sinusoidal waveform so that the THD level is below the limits of international standards (1.57% <5%). Furthermore, the voltage balancing control is effectively achieved in the model.

ACKNOWLEDGMENT

This work was supported by smart Grids & Renewable Energies Laboratory (SRGE), Faculty of Technology, University of Tahri Mohammed Bechar.

***Authors**: Mohammed Yassine Dennai, Faculty of Science and Technology, He is a PhD in the Department of Electrical Engineering, His research activities include the Control of Electrical Systems and Renewable Energies. He is a member in Smart Grids & Renewable Energies Laboratory (SRGE) at the University of Tahri Mohammed Bechar, BP 417 Route de Kenadsa, 08000 Bechar, Algeria, E-mail: dennaimoh@yahoo.fr; Hamza Tedjini, Professor of Electrical Engineering, He is a member in Smart Grids & Renewable Energies Laboratory (SRGE) at the University of Tahri Mohammed Bechar, BP 417 Route de Kenadsa, 08000 Bechar, Algeria, E-mail: tedjini_h@yahoo.fr; Abdelfatah Nasri, Professor of Electrical Engineering, He is a member in Smart Grids & Renewable Energies Laboratory (SRGE) at the University of Tahri Mohammed Bechar, BP 417 Route de Kenadsa, 08000 Bechar, Algeria, E-mail:nasriab1978@yahoo.fr; Djamel Taibi, Professor in Ouargla University, Department of electrical engineering. His research interests are modeling, design and control of the renewable energ systems, E-mail:taibi.djamel@univ-ouargla.dz; The correspondence address is: dennaimoh@yahoo.fr*

REFERENCES

[1] J. Rodriguez, J. Pontt, P. Cortes, and R. Vargas, "Predictive control of a three-phase neutral point clamped inverter," in Proc. *IEEE 36th PESC*, 2005, pp. 1364–1369.

[2] D. Rekioua , E. Matagne, Optimization of Photovoltaic Power Systems: Modelization, simulation and control , *Springer Verlag London* 2012.
[3] A. Calle-Prado et al., “Model predictive current control of grid-connected neutral-point-clamped converters to meet low-voltage ride-through requirements,” *IEEE Trans. Ind. Electron*., vol. 62, no. 3, pp. 1503–1514, Mar. 2015.
[4] Jose Rodriguez, Steffen Bernet, Peter K. Steimer, Ignacio E. Lizama, “A Survey on Neutral-Point-Clamped Inverters”, *IEEE Trans. Ind. Electron*., Vol. 57, No. 7, pp. 2219-2230, Jul. 2010.
[5] Sixing Du, Jinjun Liu, Jiliang Lin, “Hybrid Cascaded H-brigde converter for Harmonic Current Compensation”, *IEEE Trans. Power Electron*., Vol. 28, No. 5, pp. 2170-2179, May 2013.
[6] Hill CA, Such MC, Chen D, Gonzalez J, Grady WM. Battery energy storage for enabling integration of distributed solar power generation. *IEEE Transactions on the smart grid*. 2012 Jun;3(2):850-7.
[7] N. Femia, G. Petrone, G. Spagnuolo, and M. Vitelli, “A technique for improving P&O MPPT performances of double-stage grid-connected photovoltaic systems” ,*IEEE Trans. Ind. Electron*., vol. 56, no. 11,pp. 4473–4482, Nov. 2009.
[8] T. Esram and P. L. Chapman, “Comparison of photovoltaic array maximum power point tracking techniques”, *IEEE Trans. Energy Convers*., vol. 22, no. 2, pp. 439–449, Jun. 2007.
[9] G N. Femia, G. Petrone, G. Spagnuolo, M. Vitelli, “Optimization of perturb and observe maximum power point tracking method,” *IEEE Trans. Power Electron*., vol. 20, no. 4, pp. 963–973, Jul. 2005.
[10] A. Calle-Prado, S. Alepuz, J. Bordonau, J. Nicolas-Apruzzese, P. Cortes, and J. Rodriguez, "Model Predictive Current Control of Grid-Connected Neutral-Point-Clamped Converters to Meet Low-Voltage Ride-Tbrougb Requirements ," *IEEE Transactions on Industrial Electron ics*, vol. 62, pp. 1503-1514, 2015.
[11] A. Bouzidi, M. L. Bendaas, S. Barkat and M. Bouzidi, “Sliding mode control of three-level NPC inverter based grid-connected photovoltaic system”, 2017 *6th International Conference on Systems and Control (ICSC)*, Batna, 2017, pp. 354-359.
[12] A. Zorig, M. Belkheiri, S. Barkat and A. Rabhi, “Control of three-level NPC inverter based grid connected PV system”, *2015 3rd International Conference on Control, Engineering & Information Technology (CEIT)*, Tlemcen, 2015, pp. 1-6.
[13] T. Taufik, T. Wong, O. Jong, and D. Dolan, “Design and simulation of multiple-input single-output DC-DC converter,” in 2012 Ninth *International Conference on Information Technology-New Generations*, 2012, pp. 478–483.
[14] A. Calle-Prado, S. Alepuz, J. Bordonau, J. Nicolas-Apruzzese, P. Cortés and J. Rodriguez, “Model Predictive Current Control of Grid-Connected Neutral-Point-Clamped Converters to Meet Low-Voltage Ride-Through Requirements”, *in IEEE Transactions on Industrial Electronics*, vol. 62, no. 3, pp. 1503-1514, March 2015.
[15] A. Rezvani, M. Izadbakhsh, and M. Gandomkar, “Microgrid dynamic responses enhancement using artificial neural network-genetic algorithm for photovoltaic system and fuzzy controller for high wind speeds,” *International Journal of Numerical Modelling: Electronic Networks, Devices and Fields*, vol. 29, no. 2, pp. 309–332, 2016.
[16] M. R. Vincheh, A. Kargar, and G. A. Markadeh, “A hybrid control method for maximum power point tracking (MPPT) in photovoltaic systems,” *Arabian Journal for Science and Engineering*, vol. 39, no. 6, pp. 4715–4725, 2014.
[17] R. Ramaprabha, V. Gothandaraman, K. Kanimozhi, R. Divya, and B. L. Mathur, “Maximum power point tracking using GA-optimized artificial neural network for solar PV system,” *in 2011 1st International Conference on Electrical Energy Systems*, 2011, pp. 264–268.
[18] J. Yang and V. Honavar, “Feature subset selection using a genetic algorithm,” *in Feature extraction, construction and selection, Springer*, 1998, pp. 117–136.
[19] K. Xu and S. Liu, “Speed Sensorless Control with ANN and Fuzzy PI Adaptation Mechanism for Induction Motor Drive,” *Sensors & Transducers*, vol. 158, no. 11, p. 302, 2013.
[20] E. Irmak and N. Güler, “Model predictive control of grid-tied three level neutral point clamped inverter integrated with a double layer multi-input single output DC/DC converter,” *in 2018 IEEE 12th International Conference on Compatibility, Power Electronics and Power Engineering (CPE-POWERENG 2018)*, 2018, pp. 1–6.
[21] P. Q. Dzung, N. D. Tuyen, N. T. Tien, and N. C. Viet, “Model predictive current control for T-type NPC inverter using new on-line inductance estimation method,” *in 2016 IEEE Region 10 Conference (TENCON)*, 2016, pp. 316–321.
[22] Y. A. AMOR, F. HAMOUDI, and A. KHELDOUN, “Three-phase Three-level Inverter Grid-tied PV System with Fuzzy Logic Control based MPPT,” *Algerian Journal of Signals and Systems*, vol. 3, no. 3, pp. 96–105, 2018.
[23] S. Janous, D. Janik, T. Kosan, P. Kamenickỳ, and Z. Peroutka, “Comparative study of vector PWM and FS-MPC for 3-level Neutral Point Clamped converter,” *in Proceedings of the 16th International Conference on Mechatronics-Mechatronika 2014*, 2014, pp. 158–163.
[24] A. M. Dadu, T. K. Soon, S. Mekhilef, and M. Nakaoka, “Lyapunov law based model predictive control scheme for grid connected three phase three level neutral point clamped inverter,” *in 2017 IEEE 3rd International Future Energy Electronics Conference and ECCE Asia (IFEEC 2017-ECCE Asia)*, 2017, pp. 512–516.
[25] Y. Yang, H. Wen, M. Fan, M. Xie, and R. Chen, “Fast finite-switching-state model predictive control method without weighting factors for T-type three-level three-phase inverters,” *IEEE Transactions on Industrial Informatics*, vol. 15, no. 3, pp. 1298–1310, 2018.
[26] T. C. Y. Wang, Z. Ye, G. Sinha, and X. Yuan, “Output filter design for a grid-interconnected three-phase inverter,” PESC Rec. - IEEE Annu. Power Electron. Spec. Conf., vol. 2, pp. 779–784, 2003.